Supplemental Materials

Molecular Biology of the Cell

Reck et al.

Supplementary Materials-Reck et al.

Supplemental Table 1. Retrograde IFT motor subunits in *Chlamydomonas* and humans
Supplemental Table 2. *Chlamydomonas* strains used in this study
Supplemental Table 3. Antibodies used in this study

Figure S1. Strategy used to identify strains that express reduced levels of D1bLIC.
Figure S2. Flagellar length distributions in WT and *d1blic* mutant cells.
Figure S3. Movement of D1bLIC-GFP observed by TIRF microscopy in the presence and absence of the endogenous D1bLIC subunit.
Figure S4. Transport of IFT particles observed by DIC microscopy in different retrograde mutants.

Supplemental Video 1. IFT in a WT cell immobilized in agarose and observed by DIC microscopy as shown in Figure 2A.
Supplemental Video 2. IFT in a *RNAi-A* strain immobilized in agarose and observed by DIC microscopy as shown in Figure 2A.
Supplemental Video 3. IFT in a *d1blic* strain immobilized in agarose and observed by DIC microscopy as shown in Figure 4A.
Supplemental Video 4. IFT in a *d1blic::D1bLIC-GFP* strain immobilized in agarose and observed by DIC microscopy using an AxioCam MRm camera at ~25 f/s as shown in Figure 4E.
Supplemental Video 5. IFT in a *d1blic::D1bLIC-GFP* strain immobilized by EGTA and observed by TIRF microscopy using a QuantEM 512SC camera at ~16 f/s as shown in Figure 4E.
Supplemental Video 6. IFT in a *d1bLIC::D1bLIC-GFP* strain immobilized by EGTA and observed by TIRF microscopy followed by photobleaching of one flagellum as shown in Figure 4H.
Supplemental Video 7. IFT in a *pf18::D1bLIC-GFP* strain observed by TIRF microscopy as shown in Figure S3.
Supplemental Video 8. IFT in a *pf28-pf9-2 E8::D1bLIC-GFP* strain observed by TIRF microscopy as shown in Figure S3.
Supplemental Video 9. IFT in a *fla24* strain observed by DIC microscopy as shown in Figure S4.
Supplemental Video 10. IFT in a *fla2* strain observed by DIC microscopy as shown in Figure S4.
Supplemental Video 11. IFT in *a fla14* strain observed by DIC microscopy as shown in Figure S4.

Supplemental References

Supplemental Table 1. Retrograde IFT motor subunits in *Chlamydomonas* and humans

C. reinhardtii	*H. sapiens*	References
Heavy chain (HC)		
DHC1b	DYNC2H1	Pazour et al., 1999, Porter et al., 1999
Intermediate chain (IC)		
D1bIC1/FAP163	WDR60	Patel-King et al., 2013; Asante et al., 2014
D1bIC2/FAP133	WDR34	Rompolas et al., 2007; Asante et al., 2014
Light intermediate chain (LIC)		
D1bLIC	DYNC2LI1	Grissom et al., 2002; Mikami et al., 2002; Perrone et al., 2003; Hou and Witman, 2004
Light chain (LC)		
TCTEX1	DYNLT1/T3	Asante et al., 2014; Schmidts et al., 2015
TCTEX2b	TCTEX1D2	DiBella et al., 2004; Asante et al., 2014; Schmidts et al., 2015
LC7b/LC7a?	DYNLRB1/B2	Asante et al., 2014; Schmidts et al., 2015
LC8	DYNLL1/LL2	Pazour et al., 1998; Asante et al., 2014; Schmidts et al., 2015

Supplemental Table 2. *Chlamydomonas* strains used in this study

Strain	CC number	Reference
Wild-type strains		
137c, *mt+* (*nit1 nit2*)	CC-125	Harris, 2009
137c*, mt-* (*nit1 nit2 agg1*)	CC-124	Harris, 2009
21 gr, *mt+*	CC-1690	Sager, 1955
A54 e18, *mt+* (*sr1 ac17 nit1*)	CC-2929	Schnell et al., 1993
arg7-2, mt-	CC-1820	Loppes, 1969
Motility mutants		
pf18, mt+	CC-1036	Warr et al., 1966
pf9-2 pf28 E8, mt+	CC-3903	Porter et al., 1992
***DHC1b* mutants**		
stf1-1 (T3B8)	CC-3915	Porter et al., 1999
stf1-2 (3B12)	CC-3916	Porter et al., 1999
dhc1b-1, mt+	CC-3711	Pazour et al., 1999
dhc1b-3, mt+	CC-4422	Engel et al., 2012
dhc1b-3, mt-	CC-4423	Engel et al., 2012
fla24, mt-	CC-3866	Iomini et al., 2001
***D1bLIC* related**		
d1blic-RNAi-A mt+ (4e11)	CC-4491	this study
d1blic-RNAi-B mt+ (4a2)	CC-4492	this study
d1blicΔ mt+ (T8D9*)	CC-4487	this study
d1blicΔ mt+(TBD9*)	CC-4053	Hou et al., 2004
d1blicΔ mt- (YH43)	CC-4054	Hou et al., 2004
d1blic::D1bLIC-GFP mt+ (13D)	CC-4488	Rescue of T8D9, this study
d1blic::D1bLIC-GFP mt-	CC-4574	Rescue of YH43, this study
pf18::D1bLIC-GFP mt+	CC-4489	this study
pf9-2 pf28 E8::D1bLIC-GFP mt+(A4)	CC-4490	Porter et al., 1992; this study
***LC8* related**		
fla14-1, mt+	CC-3937	Pazour et al., 1998
fla14-2, mt+	CC-3938	Pazour et al., 1998
fla14-1::FLA14, mt -	CC-3939	Pazour et al., 1998
IFT mutants		
fla2, mt-	CC-1390	Huang et al., 1977

*T8D9 and TBD9 are presumed to be the same strain, but the name changed in transit between different laboratories. Both contain an uncharacterized paralyzed flagellar mutation (this study).

Supplemental Table 3. Antibodies used in this study

Antigen	Dilution for Blot	Reference/Source
Retrograde motor		
DHC1b	1:3000-1:5000	Perrone et al., 2003
D1bLIC	1:20000	Perrone et al., 2003
D1bIC2/FAP133	1:20000	This study
LC8 (R4058)	1:50	King and Patel-King, 1995
Anterograde motor		
KAP	1:1000-1:10000	Mueller et al., 2005
FLA10 (neck)	1:5000-1:20000	Cole et al., 1998
IFT particle subunits		
IFT172	1:3000	Cole et al., 1998
IFT139	1:3000	Cole et al., 1998
Other		
IC2/IC69	1:20000	Sigma D6168
a-Tubulin	1:1000-1:2000	Sigma T-5168
AOX	1:3000-1:15000	Agrisera AS06 152
RSP16	1:10000-1:20000	Yang et al., 2005
PKD2	1:2000	Huang et al., 2007
GFP	1:5000	Covance MMS-118P

Supplemental references

Asante, D., Stevenson, N.L., and Stephens, D.J. (2014). Subunit composition of the human cytoplasmic dynein-2 complex. J Cell Sci *127*, 4774-4787.

Cole, D.G., Diener, D.R., Himelblau, A.L., Beech, P.L., Fuster, J.C., and Rosenbaum, J.L. (1998). *Chlamydomonas* kinesin-II-dependent intraflagellar transport (IFT): IFT particles contain proteins required for ciliary assembly in *Caenorhabditis elegans* sensory neurons. J Cell Biol *141*, 993-1008.

DiBella, L.M., Smith, E.F., Patel-King, R.S., Wakabayashi, K., and King, S.M. (2004). A novel Tctex2-related light chain is required for stability of inner dynein arm I1 and motor function in the *Chlamydomonas* flagellum. J Biol Chem *279*, 21666-21676.

Engel, B.D., Ishikawa, H., Wemmer, K.A., Geimer, S., Wakabayashi, K., Hirono, M., Craige, B., Pazour, G.J., Witman, G.B., Kamiya, R., and Marshall, W.F. (2012). The role of retrograde intraflagellar transport in flagellar assembly, maintenance, and function. J Cell Biol *199*, 151-167.

Grissom, P.M., Vaisberg, E.A., and McIntosh, J.R. (2002). Identification of a novel light intermediate chain (D2LIC) for mammalian cytoplasmic dynein 2. Mol Biol Cell *13*, 817-829.

Harris, E. (2009). The *Chlamydomonas* Sourcebook: Introduction to Chlamydomonas and Its Laboratory Use. Academic Press: San Diego, CA.

Hou, Y., Pazour, G.J., and Witman, G.B. (2004). A dynein light intermediate chain, D1bLIC, is required for retrograde intraflagellar transport. Mol Biol Cell *15*, 4382-4394.

Huang, B., Rifkin, M.R., and Luck, D.J. (1977). Temperature-sensitive mutations affecting flagellar assembly and function in *Chlamydomonas reinhardtii*. J Cell Biol *72*, 67-85.

Huang, K., Diener, D.R., Mitchell, A., Pazour, G.J., Witman, G.B., and Rosenbaum, J.L. (2007). Function and dynamics of PKD2 in *Chlamydomonas reinhardtii* flagella. J Cell Biol *179*, 501-514.

Iomini, C., Babaev-Khaimov, V., Sassaroli, M., and Piperno, G. (2001). Protein particles in *Chlamydomonas* flagella undergo a transport cycle consisting of four phases. J Cell Biol *153*, 13-24.

King, S.M., and Patel-King, R.S. (1995). The M(r) = 8,000 and 11,000 outer arm dynein light chains from *Chlamydomonas* flagella have cytoplasmic homologues. J Biol Chem *270*, 11445-11452.

Loppes, R. (1969). A new class of arginine-requiring mutants in *Chlamydomonas reinhardii*. Mol. & Gen. Genet. *104*, 172-177.

Mikami, A., Tynan, S.H., Hama, T., Luby-Phelps, K., Saito, T., Crandall, J.E., Besharse, J.C., and Vallee, R.B. (2002). Molecular structure of cytoplasmic dynein 2 and its distribution in neuronal and ciliated cells. J Cell Sci *115*, 4801-4808.

Mueller, J., Perrone, C.A., Bower, R., Cole, D.G., and Porter, M.E. (2005). The FLA3 KAP subunit is required for localization of kinesin-2 to the site of flagellar assembly and processive anterograde intraflagellar transport. Mol Biol Cell *16*, 1341-1354.

Patel-King, R.S., Gilberti, R.M., Hom, E.F., and King, S.M. (2013). WD60/FAP163 is a dynein intermediate chain required for retrograde intraflagellar transport in cilia. Mol Biol Cell *24*, 2668-2677.

Pazour, G.J., Wilkerson, C.G., and Witman, G.B. (1998). A dynein light chain is essential for the retrograde particle movement of intraflagellar transport (IFT). J Cell Biol *141*, 979-992.

Pazour, G.J., Dickert, B.L., and Witman, G.B. (1999). The DHC1b (DHC2) isoform of cytoplasmic dynein is required for flagellar assembly. J Cell Biol *144*, 473-481.

Perrone, C.A., Tritschler, D., Taulman, P., Bower, R., Yoder, B.K., and Porter, M.E. (2003). A novel dynein light intermediate chain colocalizes with the retrograde motor for intraflagellar transport at sites of axoneme assembly in *Chlamydomonas* and mammalian cells. Mol Biol Cell *14*, 2041-2056.

Porter, M.E., Power, J., and Dutcher, S.K. (1992). Extragenic suppressors of paralyzed flagellar mutations in

Chlamydomonas reinhardtii identify loci that alter the inner dynein arms. J. Cell Biol. *118*, 1163-1176.

Porter, M.E., Bower, R., Knott, J.A., Byrd, P., and Dentler, W. (1999). Cytoplasmic dynein heavy chain 1b is required for flagellar assembly in *Chlamydomonas*. Mol. Biol. Cell *10*, 693-712.

Rompolas, P., Pedersen, L.B., Patel-King, R.S., and King, S.M. (2007). *Chlamydomonas* FAP133 is a dynein intermediate chain associated with the retrograde intraflagellar transport motor. J Cell Sci *120*, 3653-3665.

Sager, R. (1955). Inheritance in the Green Alga *Chlamydomonas Reinhardi*. Genetics *40*, 476-489.

Schmidts, M., Vodopiutz, J., Christou-Savina, S., Cortes, C.R., McInerney-Leo, A.M., Emes, R.D., Arts, H.H., Tuysuz, B., D'Silva, J., Leo, P.J., Giles, T.C., Oud, M.M., Harris, J.A., Koopmans, M., Marshall, M., Elcioglu, N., Kuechler, A., Bockenhauer, D., Moore, A.T., Wilson, L.C., Janecke, A.R., Hurles, M.E., Emmet, W., Gardiner, B., Streubel, B., Dopita, B., Zankl, A., Kayserili, H., Scambler, P.J., Brown, M.A., Beales, P.L., Wicking, C., UK10K, Duncan, E.L., and Mitchison, H.M. (2013). Mutations in the gene encoding IFT dynein complex component WDR34 cause Jeune asphyxiating thoracic dystrophy. Am J Hum Genet *93*, 932-944.

Schmidts, M., Hou, Y., Cortes, C.R., Mans, D.A., Huber, C., Boldt, K., Patel, M., van Reeuwijk, J., Plaza, J.M., van Beersum, S.E., Yap, Z.M., Letteboer, S.J., Taylor, S.P., Herridge, W., Johnson, C.A., Scambler, P.J., Ueffing, M., Kayserili, H., Krakow, D., King, S.M., Beales, P.L., Al-Gazali, L., Wicking, C., Cormier-Daire, V., Roepman, R., Mitchison, H.M., Witman, G.B., and Uk10K. (2015). TCTEX1D2 mutations underlie Jeune asphyxiating thoracic dystrophy with impaired retrograde intraflagellar transport. Nat Commun *6*, 7074.

Schnell, R.A., and Lefebvre, P.A. (1993). Isolation of the *Chlamydomonas* regulatory gene *NIT2* by transposon tagging. Genetics *134*, 737-747.

Warr, J.R., McVittie, A., Randall, J.T., and Hopkins, J.M. (1966). Genetic control of flagellar structure in *Chlamydomonas reinhardtii*. Genet. Res. Camb. *7*, 335-351.

Yang, C., Compton, M.M., and Yang, P. (2005). Dimeric novel HSP40 is incorporated into the radial spoke complex during the assembly process in flagella. Mol Biol Cell *16*, 637-648.

Supplemental Figure 1

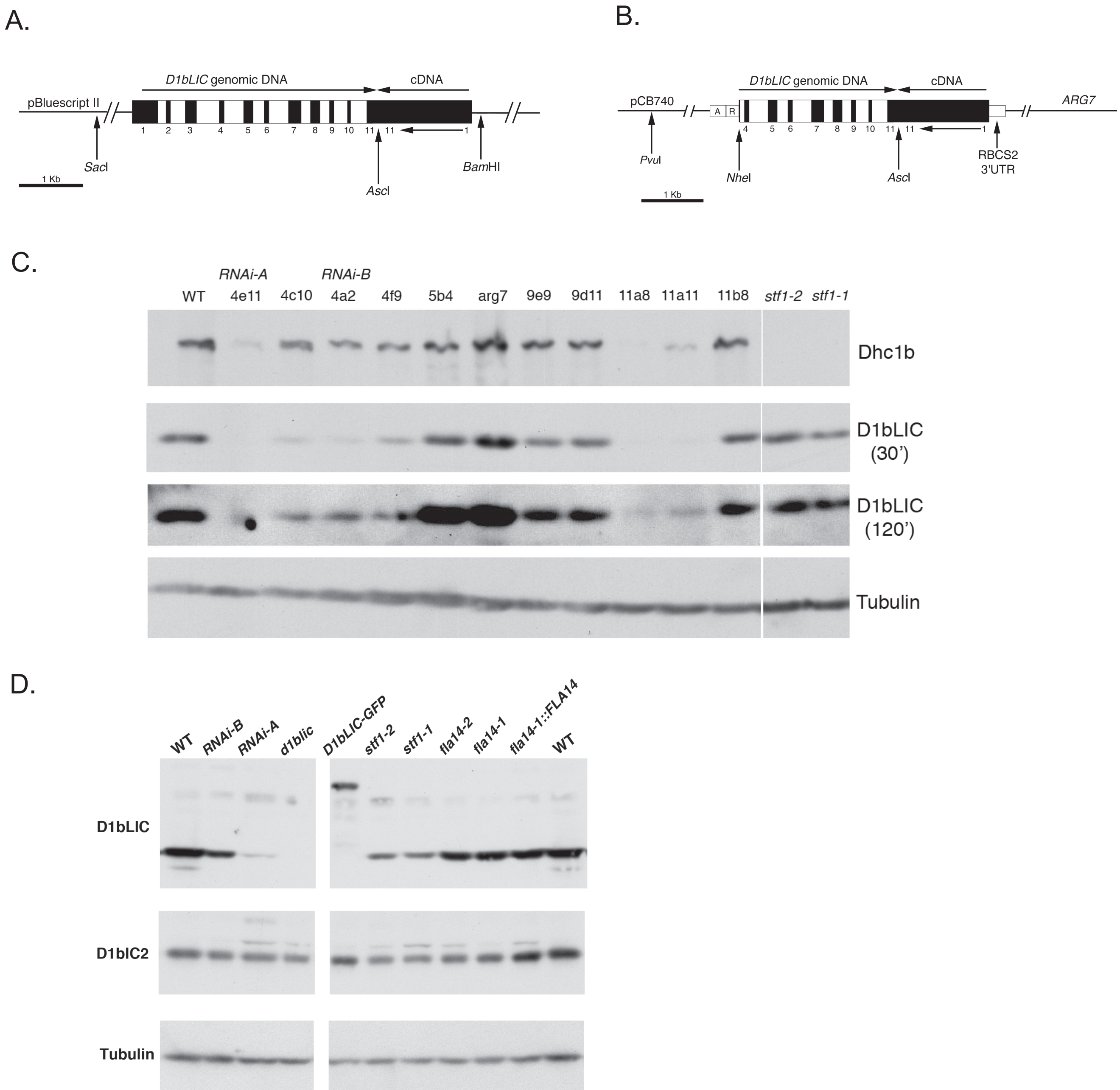

Figure S1. Strategy used to identify strains that express reduced levels of D1bLIC. The two constructs used to reduce expression of D1bLIC are shown here. **(A)** A cDNA containing exons 1-11 was inserted in reverse orientation into a genomic *D1bLIC* clone containing exons 1-11 and introduced into a WT strain (A54 e18) by co-transformation with pSI103. **(B)** A second *D1bLIC* antisense construct linked to the *ARG7* gene was introduced into an *arg7* strain. **(C)** Western blot of cell extracts probed with antibodies to DHC1b, D1bLIC, and tubulin identified several transformants that express reduced amounts of D1bLIC. Two different exposures of the D1bLIC blot are shown. Tubulin served as a loading control. The *stf* strains are *dhc1b* null strains (Porter et al., 1999). The 4e11 (*RNAi-A*) and 4a2 (*RNAi-B*) strains were selected for further study. **(D)** A Western blot of cell extracts probed with antibodies to D1bLIC, D1bIC2 (FAP133), and tubulin (loading control).

Supplemental Figure 2

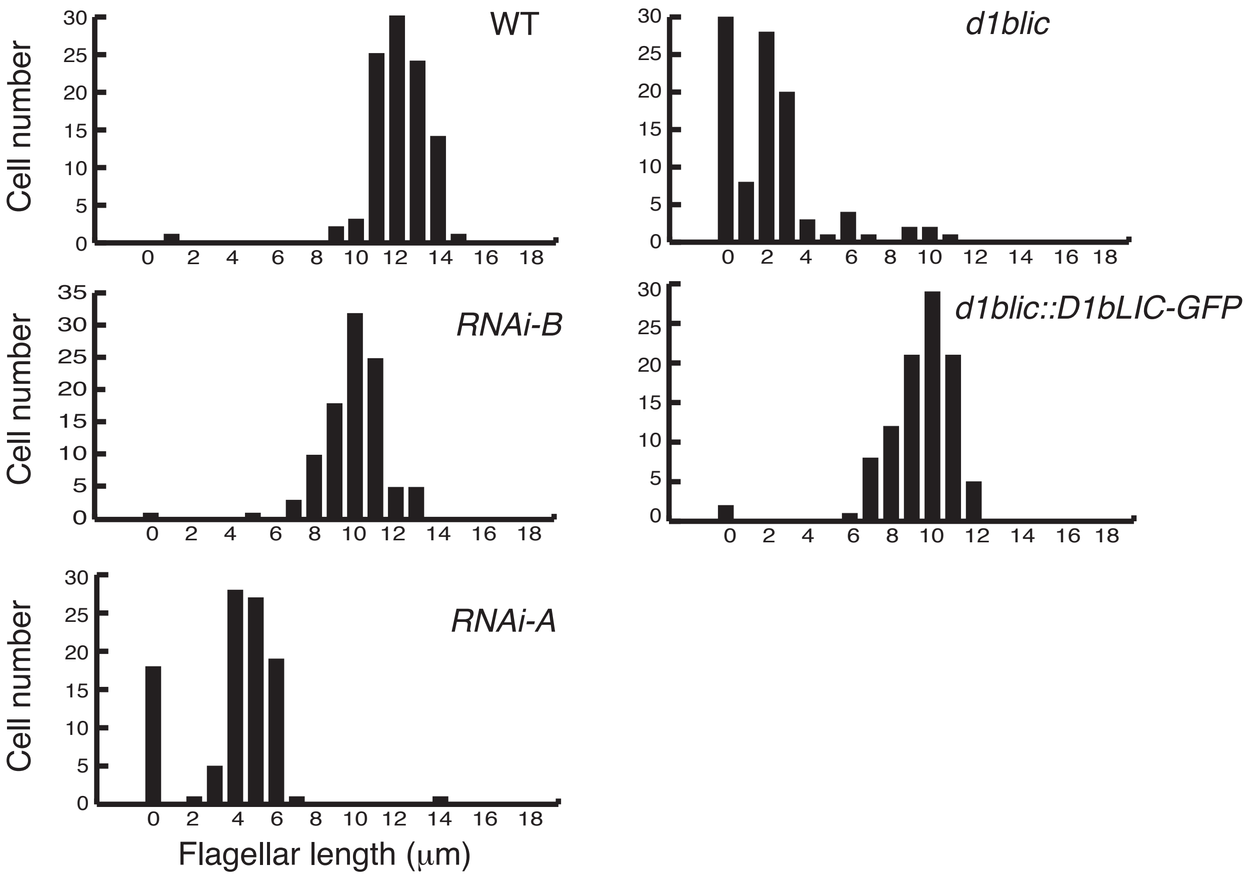

Figure S2. Flagellar length distributions in WT and *d1blic* mutant cells. The number and length of flagella present in a population of approximately 100 cells are shown, including cells with no flagella.

Supplemental Figure 3

A.

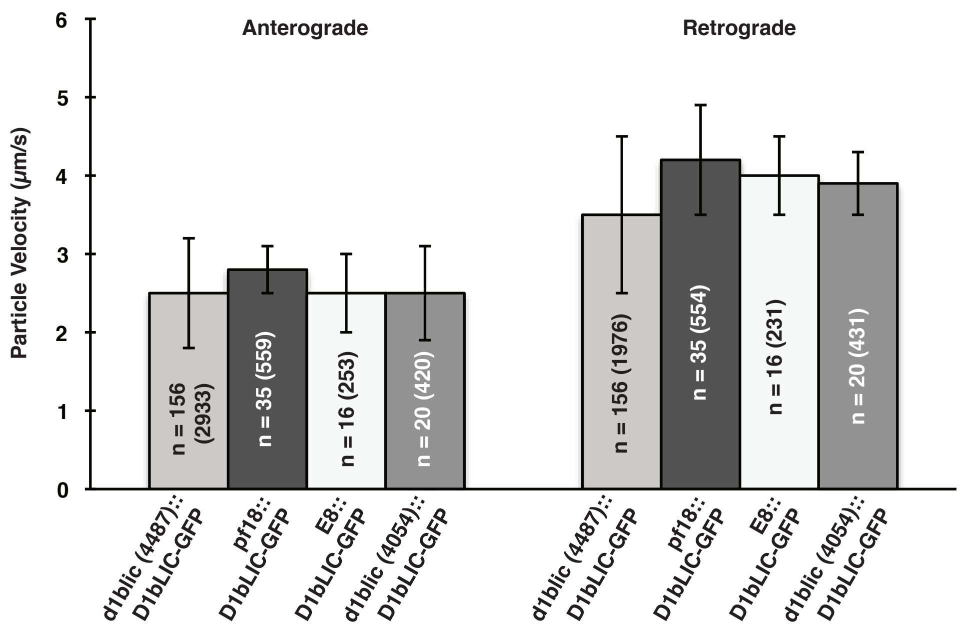

B.

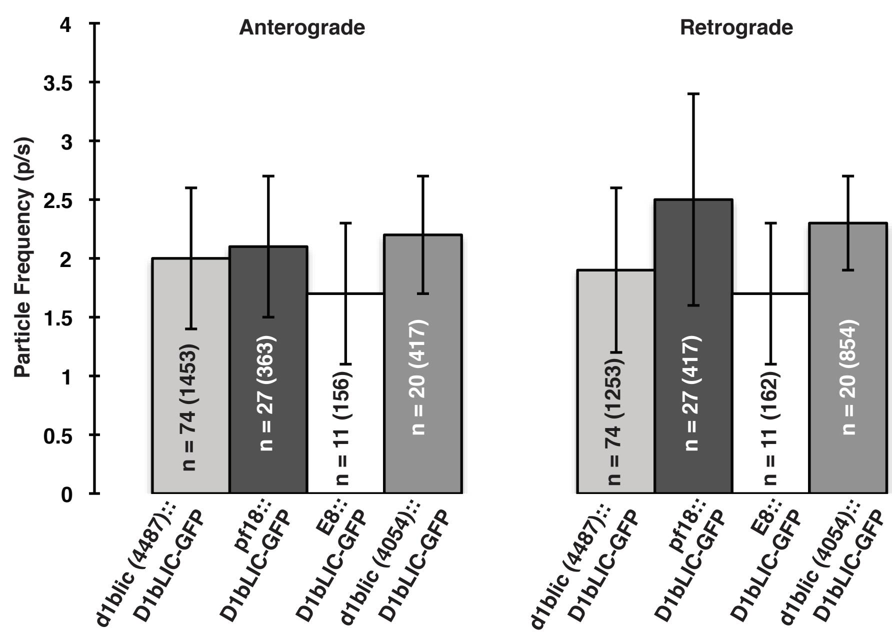

Figure S3. Movement of D1bLIC-GFP observed by TIRF microscopy in the presence and absence of the endogenous D1bLIC subunit. Two versions of the *d1blic* mutant (CC-4487 and CC-4054) and two partially paralyzed strains with an endogenous copy of the D1bLIC subunit (*pf18* and E8) were transformed with *D1bLIC-GFP*. The movement of D1bLIC-GFP particles in flagella was tracked by TIRF microscopy, and kymographs were analyzed as shown here. **(A)** Average particle velocity, n = flagella and particles measured. **(B)** Average particle frequency, n = flagella and particles measured. Although small differences in IFT particle velocity and frequency were observed between strains, the presence or absence of the endogenous D1bLIC subunit did not significantly alter the observed frequency of D1bLIC-GFP labeled particles. See Videos S7, S8.

Supplemental Figure 4.

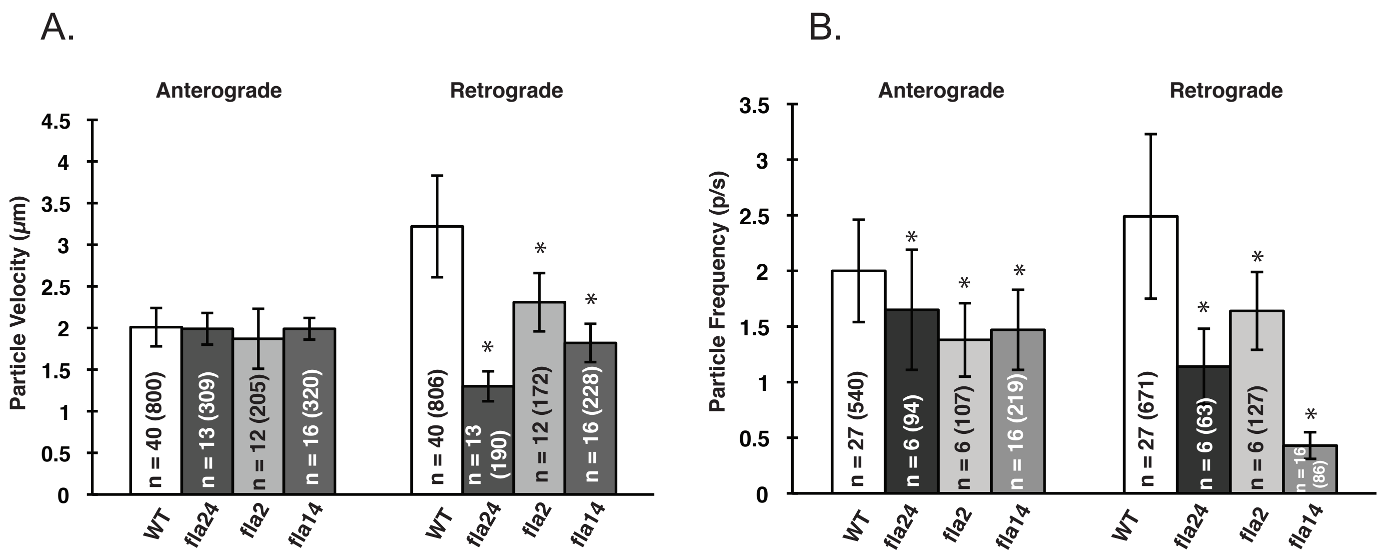

Figure S4. Transport of IFT particles observed by DIC microscopy in different retrograde mutants. The transport of IFT particles in flagella of WT and three retrograde mutants (*fla2, fla24,* and *fla14)* was analyzed by DIC microscopy at the permissive temperature. **(A)** Average particle velocity, n = number of flagella and particles. **(B)** Average particle frequency, n = number of flagella and particles. Asterisks indicate particle velocities or frequencies that were significantly different from WT (P<0.05). See Videos S9-S11.